



25th DAAAM International Symposium on Intelligent Manufacturing and Automation, DAAAM
2014

Dynamic Analysis of Stewart Platform by Bond Graphs

Vjekoslav Damic^a, Maida Cohodar^{b*}

^aUniversity of Dubrovnik, Ciria Carica 4, Dubrovnik 20000, Croatia

^bFaculty of Mechanical Engineering, University of Sarajevo, Vilsonovo setaliste 9, Sarajevo 71000, Bosnia and Herzegovina

Abstract

Dynamic model of Stewart platform was developed using bond graph technique in the paper. Stewart platform has simple, compact structure with high stiffness, high strength-to-weight ratio that make it very desirable in manufacturing technology. Due to closed loop structure and kinematic constraints, dynamic analysis of such systems is rather complicated. The paper proposes a general, object oriented modelling formulation based on bond graph component model approach to develop dynamic model of a hexapod system. Model is developed and simulations were carried out using software package BondSim. Dynamic model is generated in form of differential-algebraic equation (DAEs) and solved by BondSim.

© 2015 The Authors. Published by Elsevier Ltd. This is an open access article under the CC BY-NC-ND license (<http://creativecommons.org/licenses/by-nc-nd/4.0/>).

Peer-review under responsibility of DAAAM International Vienna

Keywords: Multibody system dynamic; Stewart platform; Bond graphs; Component model approach

1. Introduction

Owing to closed kinematic structure, Stewart platform (SP) mechanism has more stiffness and load-carrying capacity in comparison with mechanisms composed as open kinematic chains. Originally designed by Stewart [2] as mechanism for flight simulation, Stewart platform has used in many applications today (milling machine and high-speed machine tools, 'pick-and-place' applications, medical surgery, etc.). The basic platform structure has been slightly modified and partially improved from the original design by Stewart up to now. Gough applied linear actuated legs structure for the tire test machine. Thus, this mechanism is sometimes called Stewart-Gough platform in certain referral sources [3,14,15].

The Stewart platform consists of two rigid platforms, one is fixed to the ground and the other is moveable. It has

* Corresponding author. Tel.: +387-33-729-871; fax: +387-33-653-055.

E-mail address: cohodar@mef.unsa.ba

6 degrees of freedom (DOFs). The platforms are connected by six extendable legs. Such construction provides very good payload, high load/weight ratio with extremely good dexterity and mobility. These are the reasons why investigation of Stewart platform attracts the attention of many researches around the world. In [4] general form of Stewart platform was considered proving the existence of 3850 possible solutions of SP design, obtained by combining different kind of joints and constrains. Authors showed how to realize generalized Stewart platform in various fields.

Dynamic analysis of Stewart platform is subject of many researches that used different kinds of control strategies. In these works SP is energized in different ways. Hydraulic actuated SP is subject of research in [8] where virtual prototype of hydraulic actuated Stewart force feedback master-slave system (using PID controller) is developed using MATLAB-Simulink program. The inverse models for the system kinematics and dynamics of hydraulic actuated Stewart platform are developed using Matlab in [13]. In [12] a piezo stack actuators for effectively damping of the SP vibration was analysed. Dynamic modelling of electrically actuated SP is subject of research in [9], where Kane's equation is used for analysis of the driven torque of motors. Stewart platform, driven by permanent magnet synchrous motor, is analysed in [10].

Closed-form dynamic equations of mechanism and actuator are derived using Langrangian method and simulation is performed by using MATLAB-Simulink in [6].

Comparison of two control strategies – PID and generalized predictive control is realized in [7]. Using genetic algorithm by Matlab, the methodology for design optimization of 6 DOF active vibration isolation system based on Stewart platform is presented in [11].

Bond graph model of Stewart platform is developed in this work using program package BondSim [1]. Presented strategy is based on hierarchical component model approach. The procedure is comfortable even in the case of the complex system. Model of SP was developed using components from the program library, and creating new components. Mathematical model of SP is automatically generated during the model building phase in the form of differential algebraic equations (DAEs). Owing to velocity formulation obtained using bond graphs, generated DAE system has index 1, and is solved using modified backward differential formula (BDF) solver.

1.1. Structure of the paper

Structure of the paper is as follows. An introduction to the problem is given in section 1. The structure of the considered SP with attached coordinate frames used in the dynamic analysis is subject of the second section. Bond graph model of SP is developed and described in the third part of the paper. Results of simulation are presented in fourth part of this work.

1.2. Directions of the future investigation

The bond graph model of the Stewart platform developed will be used for future investigation: In particular, a visual model of Stewart platform will be developed using VTK C++ library. Performances and characteristics of Stewart platform will be investigated by simulations, during which communication between dynamic and visual models will be established, by two different applications: BondSim and BondSimVisual.

In addition, model of a hydraulic actuation system to power the prismatic joints should be developed applying bond graph technique. A possible control structures will be analysed to provide desired motion of the moving platform.

2. Structure of the Stewart platform

The structure of Stewart platform is shown in Fig.1. SP consists of two platforms: the fixed and the moving one. Moveable platform is connected to the fixed one by six legs. Each leg is extendable by prismatic joint. Lower part of legs is joined with fixed platform by universal joint providing two rotations. Upper part of legs is connected to the moving platform with spherical joint providing three rotations about three coordinate axes. The whole structure has 13 moving parts considered as rigid bodies. The unconstrained 13 rigid bodies have $13 \times 6 = 78$ degrees of freedom (DOFs). The structure has 6 universal joints with 2 DOFs, 6 prismatic joint with one DOF, and 6 spherical joints

with 3 DOFs. Structure has totally $6 \times (6-2) + 6 \times (6-1) + 6 \times (6-3) = 72$ constrains. This means that the moving platform has six DOFs as a unconstrained body in space.

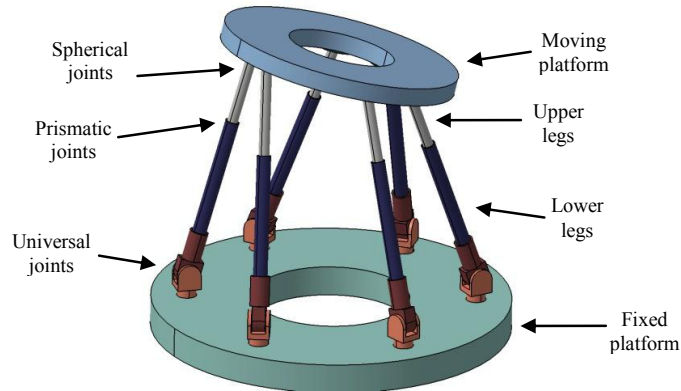


Fig. 1. Stewart platform.

Schematic representation of SP is shown in Fig.2.

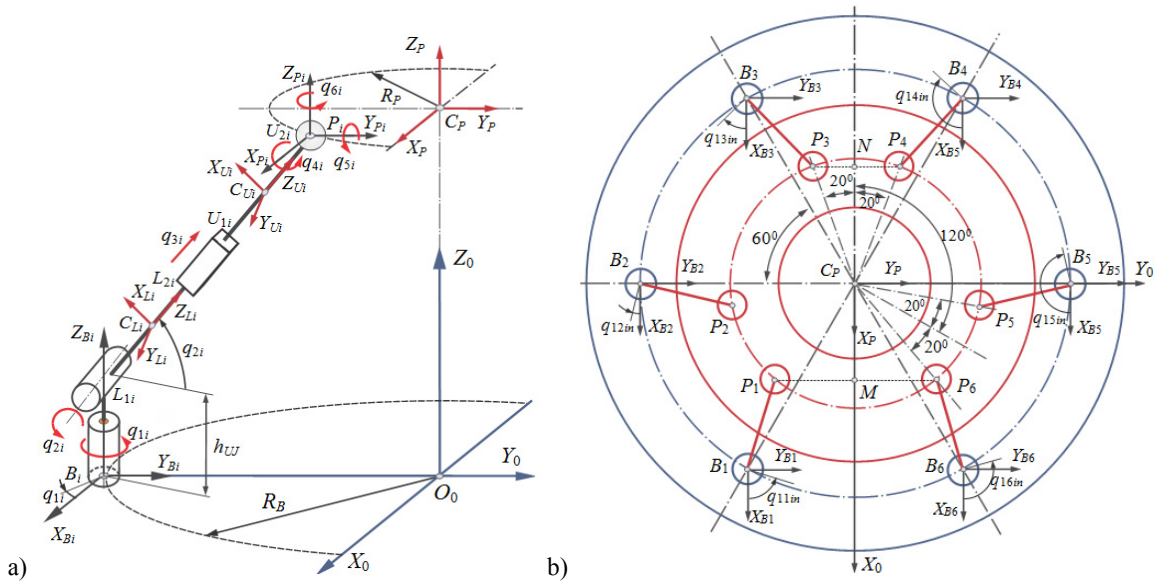


Fig. 2. (a) Scheme of the Stewart platform structure; (b) Top view on Stewart platform.

Universal joint provides two rotations – q_{1i} and q_{2i} ($i=1,2,..6$). It is realized by combination of two revolute joints. Prismatic joint provides leg extension, denoted by q_{3i} ($i=1,2,..6$). Each leg is realized as a serial kinematic chain. Structure is closed by the moving platform, connected to the upper part of the legs by the spherical joints. The inertial frame is denoted by $O_0X_0Y_0Z_0$. The frame $O_{Bi}X_{Bi}Y_{Bi}Z_{Bi}$ ($i=1,2,..6$) is attached to each universal joint, having the same orientation as the global frame. The local frames $O_{Li}X_{Li}Y_{Li}Z_{Li}$, $O_{Ui}X_{Ui}Y_{Ui}Z_{Ui}$, ($i=1,2,..6$) and $O_{Pi}X_{Pi}Y_{Pi}Z_{Pi}$, respectively, are defined with the origins at their mass center for each rigid body – the lower and upper part of legs and moving platform. Orientation of leg parts regarding to the global frame can be defined by following rotation matrices (for simplicity $\sin(\alpha)=s_\alpha$; $\cos(\alpha)=c_\alpha$ notation was used):

$$\mathbf{R}_k^0 = \begin{bmatrix} s_{q_{1i}} s_{q_{2i}} & c_{q_{1i}} & -s_{q_{1i}} c_{q_{2i}} \\ -c_{q_{1i}} s_{q_{2i}} & s_{q_{1i}} & c_{q_{1i}} c_{q_{2i}} \\ c_{q_{2i}} & 0 & s_{q_{2i}} \end{bmatrix}, \quad (k = L_i, U_i; \quad (i = 1, \dots, 6)). \tag{1}$$

Orientation of the moving platform with respect to global frame is defined by matrix:

$$\mathbf{R}_P^0 = \begin{bmatrix} \mathbf{i}_P^0 & \mathbf{j}_P^0 & \mathbf{k}_P^0 \end{bmatrix}, \tag{2}$$

where unit vectors \mathbf{i}_P^0 and \mathbf{j}_P^0 , according to Fig.2, can be defined by:

$$\mathbf{i}_P^0 = \frac{\mathbf{r}_M^0 - \mathbf{r}_N^0}{MN} = \frac{1}{2 \cdot MN} \begin{bmatrix} X_{P_1}^0 + X_{P_6}^0 - X_{P_3}^0 - X_{P_4}^0 \\ Y_{P_1}^0 + Y_{P_6}^0 - Y_{P_3}^0 - Y_{P_4}^0 \\ Z_{P_1}^0 + Z_{P_6}^0 - Z_{P_3}^0 - Z_{P_4}^0 \end{bmatrix}, \quad \mathbf{j}_P^0 = \frac{\mathbf{r}_{P_6}^0 - \mathbf{r}_{P_1}^0}{P_1 P_2} = \frac{1}{P_1 P_2} \begin{bmatrix} X_{P_6}^0 - X_{P_1}^0 \\ Y_{P_6}^0 - Y_{P_1}^0 \\ Z_{P_6}^0 - Z_{P_1}^0 \end{bmatrix}, \tag{3}$$

where $\overline{MN} = R_P \cdot (\cos(20^\circ) + \cos(40^\circ))$ and $\overline{P_1 P_6} = 2R_P \cdot \sin(40^\circ)$. Third unit vector \mathbf{k}_P^0 is vector product previously defined unit vectors:

$$\mathbf{k}_P^0 = \mathbf{i}_P^0 \times \mathbf{j}_P^0 = \begin{bmatrix} 0 & -i_{Pz}^0 & i_{Py}^0 \\ i_{Pz}^0 & 0 & -i_{Px}^0 \\ -i_{Py}^0 & i_{Px}^0 & 0 \end{bmatrix} \cdot \begin{bmatrix} j_{Px}^0 \\ j_{Py}^0 \\ j_{Pz}^0 \end{bmatrix} = \begin{bmatrix} -i_{Pz}^0 j_{Py}^0 + i_{Py}^0 j_{Pz}^0 \\ i_{Pz}^0 j_{Px}^0 - i_{Px}^0 j_{Pz}^0 \\ -i_{Py}^0 j_{Px}^0 + i_{Px}^0 j_{Py}^0 \end{bmatrix}. \tag{4}$$

3. Bond graph model of the Stewart platform

Bond graph model of Stewart platform on the system level is depicted in Fig. 3.

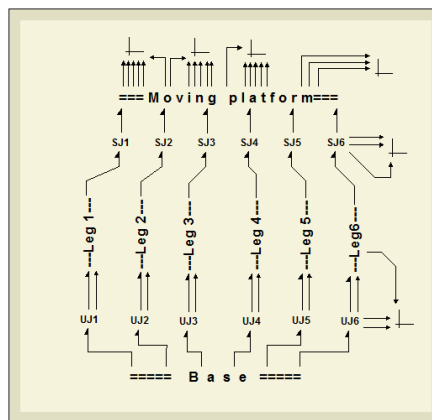


Fig. 3. Bond graph model of Stewart platform, system level.

Component **Base** represents fixed platform. This component consists of six *Source flows* **SF** for each contact points between the base and universal joints on the last level decomposition. Three of them describe linear velocity is equal zero. The other three *Source flows* provide angular velocity of lower platform is also equal zero.

Lower and upper part of legs and moving platform are considered as rigid bodies. They are realized by bond graph components of rigid body. Complete procedure how to define bond graph model of rigid body is described in [1] in detail. This component is used in [5] for modeling of hydraulic actuated crane. Bond graph models of the lower or upper part of legs are the same (Fig.4). Both parts have two connection points with rest of the system.

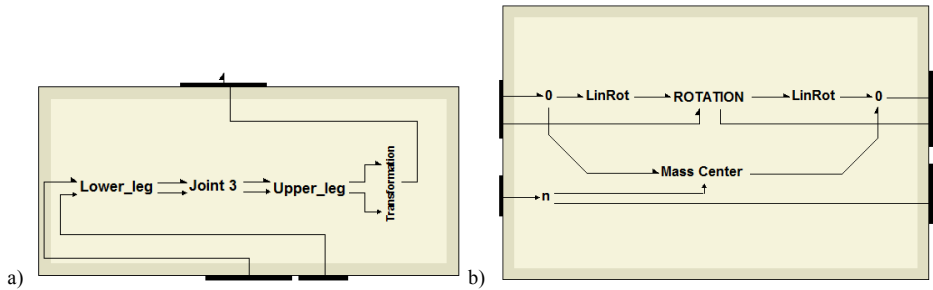


Fig. 4. Bond graph component of legs **Leg i** ($i=1,2,..6$): (a) the first level of decomposition; (b) structure of **Lower_leg** or **Upper_leg**.

Bond graph model of moving platform is depicted in Fig.5. Power is fed to platform at six connection points P_i ($i=1,6$).

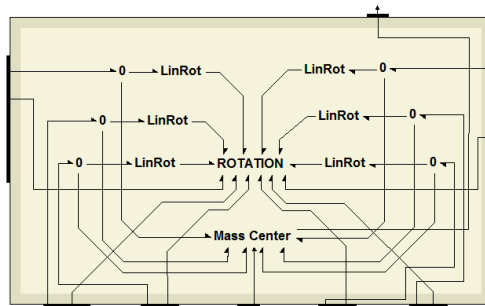


Fig. 5. Bond graph component of moving platform.

Word components **0** (two components in Fig.4b and six ones in Fig.5) consist of three components, *Flow junctions* **0**, providing the following vector relations (defined in local coordinate systems):

$$\begin{aligned}
 -\mathbf{r}_{C_{L_i},k}^{L_i} \times \boldsymbol{\omega}_{L_i}^{L_i} &= \mathbf{v}_k^{L_i} - \mathbf{v}_{C_{L_i}}^{L_i}, \quad (k = L_{1i}, L_{2i}, (i = 1,..6)), \\
 -\mathbf{r}_{C_{U_i},k}^{U_i} \times \boldsymbol{\omega}_{U_i}^{U_i} &= \mathbf{v}_k^{U_i} - \mathbf{v}_{C_{U_i}}^{U_i}, \quad (k = U_{1i}, U_{2i}, (i = 1,..6)), \\
 -\mathbf{r}_{C_P,k}^P \times \boldsymbol{\omega}_P^P &= \mathbf{v}_k^P - \mathbf{v}_{C_P}^P, \quad (k = P_i, (i = 1,..6)).
 \end{aligned}
 \tag{5}$$

Components **LinRot** represent transformations between linear and angular quantities, defined by Eq.(5). The rotation part of the body motion is described by famous Euler equations in which the rate of change of the momentum is represented by its local change and part convected by the body rotation:

$$\frac{d\mathbf{H}_j^j}{dt} + \boldsymbol{\omega}_j^j \times \mathbf{H}_j^j = \mathbf{M}_j^j, \quad (j = L_i, U_i, P; (i = 1,..6)).
 \tag{6}$$

where \mathbf{M}_j^j is the resultant moment about the body mass centre expressed in the local frame. The rotation part of rigid body motion is realized by component **ROTATION** (Figs.4b and 5). The translation part of motion can be described in the global frame by:

$$\mathbf{p}_j^0 = m_j \mathbf{I} \mathbf{v}_{C_j}^0, \quad \frac{d\mathbf{p}_j^0}{dt} = \mathbf{F}_j^0, (j = L_i, U_i, P_i; (i = 1, \dots, 6)). \tag{7}$$

where m_j is body mass and \mathbf{F}_j is resultant of the forces reduced to the mass center and defined in the global frame. It is represented by component **Mass Center** (Fig.4b and 5).

4. Numerical results

Material and geometric data of Stewart platform are given in Table 1. Coordinates of points B_i and P_i (initially posture) located on the fixed and the moving platforms in the global frame $O_0X_0Y_0Z_0$ are given in Tables 2 and 3.

Table 1. Material and geometric parameters of SP.

Parameters		Lower part of leg	Upper part of leg	Moving platform
Mass [kg]		0.045	0.016	1.001
Length [m]		0.12	0.1	
Mass mom. inertia [kgm ²]	I_{xx} [kgm ²]	6.249e-5	1.466e-5	0.003
	I_{yy} [kgm ²]	6.249e-5	1.466e-5	0.003
	I_{zz} [kgm ²]	1.148e-6	2.084e-7	0.006
R_B [m]		0.12		
R_P [m]		0.07		
h_{Lij} [m]		0.013		

Table 2. Coordinate contact points B_i ($i=1,2,\dots,6$) on the base platform in the inertial frame $O_0X_0Y_0Z_0$.

	B_1	B_2	B_3	B_4	B_5	B_6
X_{B_i}	$R_B \cdot \cos(30^0)$	0	$-R_B \cdot \cos(30^0)$	$-R_B \cdot \cos(30^0)$	0	$R_B \cdot \cos(30^0)$
Y_{B_i}	$-R_B \cdot \sin(30^0)$	$-R_B$	$-R_B \cdot \sin(30^0)$	$R_B \cdot \sin(30^0)$	R_B	$R_B \cdot \sin(30^0)$
Z_{B_i} [m]	0	0	0	0	0	0

Table 3. Coordinate contact points P_i ($i=1,2,\dots,6$) on the moving platform in the inertial frame $O_0X_0Y_0Z_0$.

	P_1	P_2	P_3	P_4	P_5	P_6
X_{P_i}	$R_P \cdot \sin(50^0)$	$R_P \cdot \sin(10^0)$	$-R_P \cdot \sin(70^0)$	$-R_P \cdot \sin(70^0)$	$R_P \cdot \sin(10^0)$	$R_P \cdot \sin(50^0)$
Y_{P_i}	$-R_P \cdot \cos(50^0)$	$-R_P \cdot \cos(10^0)$	$-R_P \cdot \cos(70^0)$	$R_P \cdot \cos(70^0)$	$R_P \cdot \cos(10^0)$	$R_P \cdot \cos(50^0)$
Z_{P_i} [m]	0.2194306	0.2194306	0.2194306	0.2194306	0.2194306	0.2194306

Table 4. Initial values of angle for the first rotation q_{1i} ($i=1,2,\dots,6$).

q_{11}	q_{12}	q_{13}	q_{14}	q_{15}	q_{16}
73.38974 ⁰	-13.38974 ⁰	-46.61026 ⁰	-133.38974 ⁰	-166.61026 ⁰	106.61026 ⁰

Initial value of second rotation of universal joint is equal for the each joint $q_{2i}=75.733^0$ ($i=1,2,\dots,6$). The upper part of the leg is retracted by 0.2 m to the prismatic joint. Four prismatic joints are actuated according to relations:

$$\dot{q}_{31} = 0.05 \cdot \cos(5t), \dot{q}_{33} = -0.05 \cdot \cos(5t), \dot{q}_{34} = -0.05 \cdot \cos(5t), \dot{q}_{36} = 0.05 \cdot \cos(5t). \tag{8}$$

The other joints enable motions compatible with their constrains. The simulation was undertaken for 5s. It has been run using the time step of 1e-4 s and absolute and relative error tolerances of 1e-8. Results are presented in Fig.6. Time histories of X_{CP} and Z_{CP} coordinates of the mass centre C_p of the moving platform are presented in Fig.6 a-b. We can see that period of oscillations is $T=2\pi/5s$. As we expected, coordinate Z_{CP} reaches maximum value $Z_{CPmax}=0.220364$ m (with amplitude of $Z_{CPmax}-Z_{CPin}=9.332e-4m$) at moment $T/4=0.3141s$, and minimum value $Z_{CPmin}=0.218459$ m at moment 0.9423s (with amplitude of $Z_{CPmin}-Z_{CPin}=-9.714e-4m$) during the first period of oscillations. Coordinate X_{Pi} and Z_{Pi} ($i=1,2,\dots,6$) with time are presented in Figs.6c-d. We can see, for instance for contact point P_1 , maximum value of $Z_{P1max}=0.2291328m$ ($Z_{P1max}-Z_{P1in}=9.7022e-3m$) is reached at $T/4=0.3141s$ and minimum value of $Z_{P1min}=0.2093716$ m ($Z_{P1min}-Z_{P1in}=-0.010m$) is reached at 0.9424s. Motions of prismatic joints q_{3i} ($i=1,3,4,6$), defined by Eqs.(8) are presented in Fig.6e. Motions compatible with their constrains for prismatic joints q_{3i} ($i=2,5$) are shown in Fig.6f.

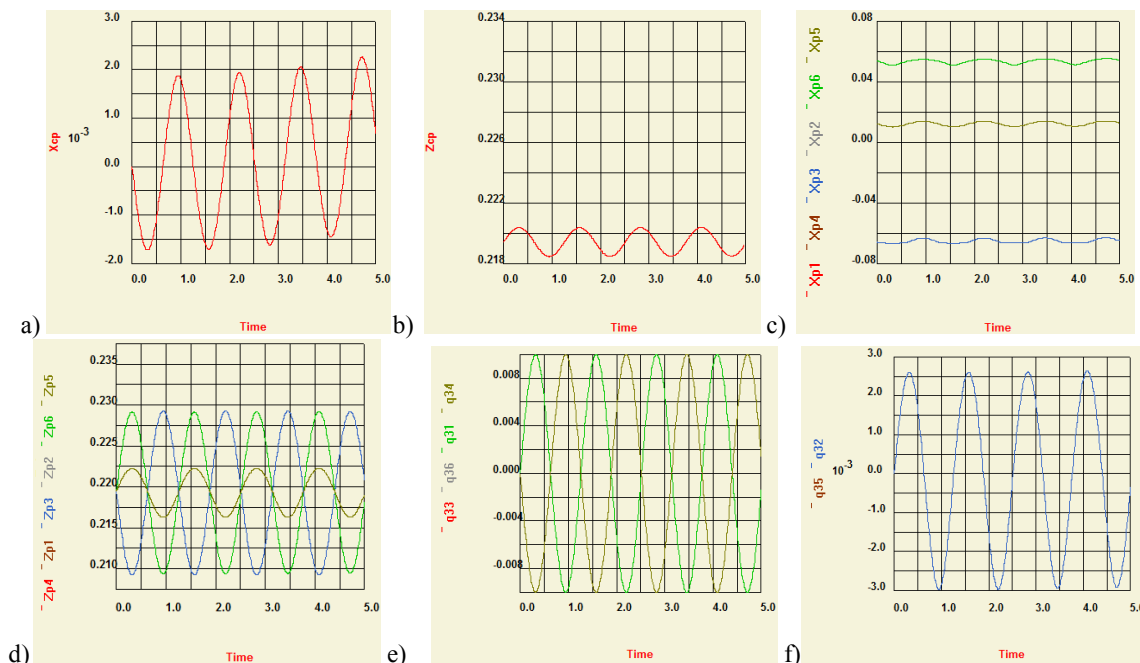


Fig. 6. Simulation results: (a) X_{CP} ; (b) Z_{CP} ; (c) X_{Pi} ($i=1,2,\dots,6$); (d) Z_{Pi} ($i=1,2,\dots,6$); (e) q_{3i} ($i=1,3,4,6$); (f) q_{3i} ($i=2,5$).

Conclusion

Dynamic model of the Stewart platform has been developed using bond graphs. The presented procedure is based on a hierarchical component model approach. It enables a systematic development of parallel manipulator structure as a hierarchical multi-level models. All manipulators parts – moving platform, lower and upper legs are treated as rigid bodies and are represented by the corresponding bond graph components. The underlying dynamical model in the form of differential-algebraic equations, is directly solved by BondSim using suitable solver.

Developed bond graph model of Stewart platform could be used as base for future investigation, e.g. analysing different control structures in order to obtain desired platform motion, development of joint actuated system, design and performance optimisation by using of visual model of SP.

Acknowledgements

This paper is realized in framework of project supported by Federal ministry of education of Bosnia and Herzegovina.

References

- [1] V. Damic, J. Montgomery, *Mechatronics by Bond Graphs*, Springer-Verlag, 2003.
- [2] D. Stewart. "A platform with six degrees of freedom", *Proc. of institute for Mechanical Engineering*, London, Vol.180, pp. 371-386, 1965.
- [3] S-K. Song, D-S. Kwon, New direct kinematic formulation of 6 D.O.F. Stewart-Gough platforms using the tetrahedron approach, *Transactions on Control, Automation and System Engineering* 4 (2002) pp.217-223.
- [4] X-S. Gao, D. Lei, Q. Liao, G-F. Zhang, Generalized Stewart platforms and their direct kinematics, *MM Research preprints*, MMRC, AMSS, Academia, Sinica, Beijing, 22 (2003) pp.64-85.
- [5] V. Damic, M. Cohodar, M. Kulenovic, Modeling and simulation of hydraulic actuated multibody systems by bond graphs, *Procedia Engineering* 69 (2014) pp.203-209.
- [6] A. El-Badawy, K. Youssef, On modeling and simulation of 6 degrees of freedom Stewart platform mechanism using multibody dynamic approach, *ECCOMAS Multibody Dynamics 2013*, 1-4 July 2013, University of Zagreb, Croatia, pp. 751-760.
- [7] Z. Bingul, O. Karahan, Dynamic modeling and simulation of Stewart platform, Serial and parallel robot manipulators – kinematics, dynamics, control and optimization, Ed. by S. Kucuk, Publisher In Tech, ISBN 978-953-51-0437-7, pp.19-42. Published online 30, March, 2012, www.intechopen.com
- [8] J. M. Rosario, D. Dumur, M. Moretti, F. Lara, A. Uribe, Supervision and control strategies of 3 DOF parallel manipulator using mechatronic approach, *Advanced strategies for robot manipulators*, Ed. By S.Ehsan Shafiei, Publisher Sciyo, ISBN 978-953-307-099-5, pp. 173-196. Published online 12, August, 2010, www.intechopen.com
- [9] H. Jingwei, Z. Dingxuan, Z. Ying, C. Yuxin, Simulation research on hydraulic Stewart force feedback Master-Slave system, *Proceeding of the 2nd International Conference on Computer Science in Electronics Engineering (ICCSEE 2013)*, Published by Atlantis Press, France, pp.2440-2443.
- [10] Q. Meng, T. Zhang, J-F. He, J-Y. Song, J-W.Han, Dynamic modeling of 6-degree-of-freedom Stewart platform driven by permanent magnet synchronous motor, *Computer&Electron.* 11(10) (2010) pp.751-761.
- [11] R.U.Baig, S.Pugazhenth, Design optimization of an active vibration isolation system, *International journal of the physical sciences* 6 (30) (2011) pp.6882-6890.
- [12] A. Bahrami, M. Tafaoli-Masoule, M. N. Bahrami, Fuzzy Logic Based Active Vibration Control of Piezoelectric Stewart Platform, *International Journal of Mechanical, Industrial Science and Engineering* Vol. 8 No. 1 (2014) pp.72-79.
- [13] A. Bose, R.Saha, K. Majumdar, D.Sanyal, A simple design approach for hydraulic Stewart platform through Matlab simulation, *Proceedings of the 1st International and 16th National Conference on Machine and Mechanism (iNaCoMM2013) India (2013)* pp.757-764.
- [14] A.-F. Behrouz, P.Lidstrom, K.Nilsson, Parametric damped vibrations of Gough-Stewart platforms for symmetric configuration, *Mechanism and Machine Theory*, 80 (2014) pp.52-69.
- [15] H.Tari, H.-J. Su, J.D.Hauenstein, Classification and complete solution of kinetostatics of a compliant Stewart-Gough platform, *Mechanism and Machine Theory* 49 (2012) pp.177-186.